STATISTICAL MODELING TO PREDICT N_2O PRODUCTION WITHIN THE HYPORHEIC ZONE BY COUPLING DENITRIFYING MICROBIAL COMMUNITY ABUNDANCE TO GEOCHEMICAL AND HYDROLOGICAL PARAMETERS

by

Tiffany Brooke Farrell

A thesis

submitted in partial fulfillment

of the requirements for the degree of

Master of Science in Hydrologic Sciences

Boise State University

May 2016

BOISE STATE UNIVERSITY GRADUATE COLLEGE

DEFENSE COMMITTEE AND FINAL READING APPROVALS

of the thesis submitted by

Tiffany Brooke Farrell

Thesis Title: Statistical Modeling to Predict N_2O Production Within the Hyporheic Zone by Coupling Denitrifying Microbial Community Abundance to Geochemical and Hydrological Parameters

Date of Final Oral Examination: 12 February 2016

The following individuals read and discussed the thesis submitted by student Tiffany Brooke Farrell, and they evaluated her presentation and response to questions during the final oral examination. They found that the student passed the final oral examination.

Kevin P. Feris, Ph.D.	Chair, Supervisory Committee
Shawn G. Benner, Ph.D.	Member, Supervisory Committee
Daniele Tonina, Ph.D.	Member, Supervisory Committee

The final reading approval of the thesis was granted by Kevin P. Feris, Ph.D., Chair of the Supervisory Committee. The thesis was approved for the Graduate College by John R. Pelton, Ph.D., Dean of the Graduate College.

DEDICATION

I would like to dedicate the work of my thesis to my family and friends who have encouraged me throughout the wonderful highs and lows of this experience and to Iseah, Guinevere, and Hank for helping me to smile through it all.

ACKNOWLEDGEMENTS

I would like to thank the NSF for financially supporting this research (grant #EAR1141690 and #EAR1141752). I am so grateful for my research partners: Annika Quick and Jeff Reeder; together we successfully conquered the vision of this project by working together as the best interdisciplinary team. You two will always be an inspiration for me. A resounding expression of gratitude goes to Kevin Feris for providing an opportunity for me to fuse my microbiological background with a hydrological perspective and preparing me with the proper tool kit to face environmental challenges. I appreciate the patience and support received from my advisors, Shawn Benner and Daniele Tonina, who helped to nourish my perspective within the physical sciences. Much appreciation for Regina Hillsberry and Christina Beeson for your hard work with this project and valuable assistance in setting up the experiment, collecting samples, and analyzing laboratory samples. A very special thank you to Laura Bond for advancing my knowledge and respect for the incredible power of statistics by dedicating your time and statistical insight to ensure the story was properly told.

ABSTRACT

The hyporheic zone (HZ) of streams can be a significant source of nitrous oxide (N_2O). However, the biogeochemical processes controlling N_2O emissions remain poorly constrained due to difficulties in obtaining high-resolution chemical, physical, and biological data from streams. We performed a large-scale flume experiment to unravel the complexities of a natural system by constraining streambed morphology, flow rate, organic carbon loading, grain size distribution, and exogenous nitrate loading while enabling regular monitoring of dissolved oxygen, pH, alkalinity, and concentrations of NO_3^-, NO_2^-, NH_4^+, and N_2O in the HZ. We employed real-time PCR (qPCR) to quantify the distribution of denitrifying functional genes (*nirS* and *nosZ*, genes that encode nitrite reductase and nitrous oxide reductases, respectively) in HZ sediment cores as a measure of denitrifying microorganism abundance. Linear and nonlinear mixed-effects models were used to elucidate specific controls on N_2O production within the HZ by coupling the distribution of denitrifying microbial communities to flow dynamics (i.e., hyporheic hydraulics and streambed morphology) and biogeochemical processes. We found that hot spots for denitrification (N_2O generation) were significantly influenced by the availability of total nitrogen only when dissolved oxygen concentrations were below 31 μmol/L. The addition of denitrifying gene abundance, *nirS*, and the interaction term between *nirS* and total nitrogen as modeling parameters significantly improved the quality of our model and predicted an increase in N_2O when *nirS* abundance was greater than 5.01×10^6 copy #/gram dry sediment. We were also able to establish a significant

negative relationship between the relative abundance of *nosZ* to *nirS* (*nosZ*/*nirS*) and N_2O generation. Our statistical model also emphasized the role of streambed morphology on N_2O generation, which is attributed to its control over the delivery and distribution of dissolved oxygen, oxidized nitrogen species, and denitrifying genes within the HZ. These results may be useful in predicting N_2O production in HZ systems and can inform mitigation strategies targeting reduction of N_2O production in HZ systems with elevated levels of reactive nitrogen.

TABLE OF CONTENTS

LIST OF TABLES

LIST OF FIGURES

STATISTICAL MODELING TO PREDICT N_2O PRODUCTION WITHIN THE HYPORHEIC ZONE BY COUPLING DENITRIFYING MICROBIAL COMMUNITY ABUNDANCE TO GEOCHEMICAL AND HYDROLOGICAL PARAMETERS

Author List: Tiffany B Farrell*[1,3], Annika M Quick[1], William Jeffery Reeder[2], Daniele Tonina[2], Shawn G Benner[1], and Kevin P Feris[3]

[1]Department of Geosciences, Boise State University, [2]Department of Civil Engineering, University of Idaho-Water Research Center and [3]Department of Biology, Boise State University

Abstract

The hyporheic zone (HZ) of streams can be a significant source of nitrous oxide (N_2O). However, the biogeochemical processes controlling N_2O emissions remain poorly constrained due to difficulties in obtaining high-resolution chemical, physical, and biological data from streams. We performed a large-scale flume experiment to unravel the complexities of a natural system by constraining streambed morphology, flow rate, organic carbon loading, grain size distribution, and exogenous nitrate loading while enabling regular monitoring of dissolved oxygen, pH, alkalinity, and concentrations of NO_3^-, NO_2^-, NH_4^+, and N_2O in the HZ. We employed real-time PCR (qPCR) to quantify the distribution of denitrifying functional genes (*nirS* and *nosZ*, genes that encode nitrite reductase and nitrous oxide reductases, respectively) in HZ sediment cores as a measure of denitrifying microorganism abundance. Linear and nonlinear mixed-effects models were used to elucidate specific controls on N_2O production within the HZ by coupling the distribution of denitrifying microbial communities to flow dynamics (i.e., hyporheic hydraulics and streambed morphology) and biogeochemical processes. We found that hot spots for denitrification (N_2O generation) were significantly influenced by the availability of total nitrogen only when dissolved oxygen concentrations were below 31 μmol/L. The addition of denitrifying gene abundance, *nirS*, and the interaction term between *nirS* and total nitrogen as modeling parameters significantly improved the quality of our model and predicted an increase in N_2O when *nirS* abundance was greater than 5.01×10^6 copy #/gram dry sediment. We were also able to establish a significant negative relationship between the relative abundance of *nosZ* to *nirS* (*nosZ*/*nirS*) and N_2O generation. Our statistical model also emphasized the role of streambed morphology on

N_2O generation, which is attributed to its control over the delivery and distribution of dissolved oxygen, oxidized nitrogen species, and denitrifying genes within the HZ. These results may be useful in predicting N_2O production in HZ systems and can inform mitigation strategies targeting reduction of N_2O production in HZ systems with elevated levels of reactive nitrogen.

Introduction

The rate at which reactive nitrogen (e.g., NO_3^- and NH_4^+) (Nr) is introduced into the biosphere has increased by an order of magnitude as anthropogenic activity expanded over the past 150 years (i.e., increased from ~15 Tg Nr/year to 160 Tg Nr/year) (Galloway et al., 2008; Seitzinger et al., 2000). This increased flux of Nr has contributed to enhanced levels of productivity in agricultural systems (Erisman et al., 2008), however it also has negative consequences. These include increased deposition of Nr to aquatic ecosystems, raising the prevalence of both eutrophication (Sutton et al., 2011) and anthropogenic emissions of the potent greenhouse gas nitrous oxide (N_2O) (Seitzinger et al., 2000). Although atmospheric concentrations of N_2O are lower than carbon dioxide (CO_2) and methane (CH_4), the global warming potential of N_2O, on an equal mass basis, is approximately 300 times greater than CO_2 and 12 times greater than CH_4 on a 100-year time scale (Forster et al., 2007) and N_2O serves a role in stratospheric ozone destruction (Ravishankara et al., 2009).

Within lotic ecosystems, Nr can drive the production of N_2O, in part, through microbial denitrification (Arango et al., 2007), an anaerobic respiratory process that couples the oxidation of reduced organic carbon to CO_2 with the successive reduction of nitrate (NO_3^-) to nitrite (NO_2^-), nitric oxide (NO), nitrous oxide (N_2O), and dinitrogen gas

(N_2) (Bothe et al., 2006). Surface waters of alluvial rivers can receive Nr from surface runoff (Carpenter et al., 1998) or through the hyporheic zone (HZ) via groundwater sources (Kellman and Hillaire-Marcel, 1998; Boulton et al., 1998). The HZ is the volume of porous saturated sediment through which surface water and underlying aquifers interact (Krause et al., 2011). Heterogeneity in the distribution of carbon, oxygen, and other terminal electron acceptors (e.g., NO_3^-, Mn^{4+}, Fe^{3+}, SO_4^{2-}, etc.) within the HZ can result in the development of an array of redox zones that support a myriad of heterotrophic processes ranging from aerobic respiration to methanogenesis (Morrice et al., 2000). The specific distribution of these processes, and therefore the potential for denitrification and N_2O production in the HZ, is driven by the amount of reactive carbon present (Zarnetske et al., 2011b), the rate of dissolved oxygen (DO) delivery to the HZ (Laursen and Seitzinger, 2004; Schaller et al., 2004), and the availability of Nr (Böhlke et al., 2009). The delivery and distribution of carbon, DO, and Nr from the surface water into and throughout the HZ is influenced by streambed morphology (Marion et al., 2002; Packman et al., 2004).

Bed form-driven solute exchange between stream flow and the HZ subsurface introduces oxygenated flow paths (Packman et al., 2004) along which respiratory processes, like denitrification, are delineated (Chapelle et al., 1995). Spatial and temporal variation in riverbed topography induce hyporheic exchange whereby downwelling flows advectively transfer surface water into the subsurface (Tonina and Buffington, 2009; Buffington and Tonina, 2009). This surface to subsurface exchange introduces dissolved oxygen (DO), nutrients such as Nr, and dissolved organic carbon (DOC) to microbial communities living on sediment surfaces (Harvey et al., 2013). If

labile carbon and heterotrophic microorganisms are present, the rate of aerobic respiration can exceed the delivery of O_2 in particle-associated microsites creating zones of anoxia (Sørensen et al., 1979; Sakita and Kusuda, 2000; Arango et al., 2007). As O_2 concentration becomes the limiting factor for aerobic respiration (e.g., between 0 and 10 μM) (Nielsen et al., 1990), and when NO_3^- and reactive carbon remain available, facultative anaerobic microbes shift their respiratory metabolism towards denitrification (Ingersoll and Baker, 1998; Kjellin et al., 2007; Kozub and Liehr, 1999; Lin et al., 2002) and transient accumulation of N_2O can occur (Morley et al., 2008; Almeida et al., 1997; Philippot et al., 2001; Bakken et al., 2012; Betlach and Tiedje, 1981; Holtan-Hartwig et al., 2000). In turn, upwelling flows bring reduced elements, such as N_2O, N_2, dissolved CO_2, etc. from the saturated sediment back into the surface water (Triska et al., 1993; Triska et al., 1989; Stanford and Ward, 1993; Malard et al., 2002).

The successive reduction of NO_3^- to N_2 is dependent on expression of the genes for nitrate (*narG*), nitrite (*nirS* or *nirK*), nitric oxide (*norI*), and nitrous oxide (*nosZ*) reductases (Bothe et al., 2006). The pathway is initiated by the membrane bound NO_3^- reductase, a three subunit enzyme (NarGHI), through which an electrochemical gradient force is generated once quinol is oxidized at NarI. This allows NO_3^- to enter the cytoplasm (in exchange for NO_2^- export to the periplasm) and subsequent electron transfer occurs through NarH to NarG, where dissimilatory reduction of NO_3^- to NO_2^- (denitrification) or to NH_3 can occur (Richardson et al., 2007) and therefore the presence of this protein is not unique to denitrification. The periplasmic nitrite reductase (Nir) reduces NO_2^- to NO and differentiates denitrifiers from other nitrate-respiring bacteria (Kandeler et al., 2006; Braker et al., 1998; Wallenstein et al., 2006). The enzymatic

expression of Nir and Nor are managed by the cell to ensure NO concentrations remain below cytotoxic levels (e.g., within a nanomolar range) (Kuňák et al., 2004). Although denitrification is a form of anaerobic respiration, Nar, Nir, and Nor can be active in the presence of O_2 (Morley et al., 2008). Elevated levels of O_2 however, inhibit activity of Nos, and can impede the environmentally significant reduction of N_2O to N_2 (Otte et al., 1996; Bakken and Dörsch, 2007; Philippot et al., 2001). Expression of Nos is also inhibited in the presence of low pH (Šimek and Cooper, 2002; Čuhel et al., 2010; Liu et al., 2014). Conversely, some denitrifying microorganisms produce N_2O as an end product because they either lack the ability to express a functional N_2O reductase (Zumft, 1997; Zumft et al., 1985) or they are missing the *nosZ* gene but retain the rest of the genes associated with denitrification (Jones et al., 2013; Wood et al., 2001; Jones et al., 2008). Even with the recent discovery of a previously unknown *nosZ* clade, the *nosZ* gene remains considerably less abundant than *nirS* genes (Jones et al., 2013). Therefore, N_2O could be lost from the HZ before being reduced to N_2 if hyporheic denitrifying communities (1) inhabit areas where either O_2 is present at levels suitable to induce denitrification but inhibit *nosZ* (e.g. ~ >23 μM O_2 (however, actual concentration is organism dependent)) (Davies et al., 1989; Coyne and Tiedje, 1990; Otte et al., 1996), (2) denitrification occurs within proximity of upwelling flows thereby limiting the reaction time and expression of nitrous oxide reductase, (3) the denitrifying community contains denitrifiers that lack the *nosZ* gene or are in low relative abundance compared to the total denitrifying community, or (4) some combination of these events. The extent to which these events take place within the HZ and could account for the estimated 10% of global

anthropogenic N_2O emissions (0.68 Tg N-N_2O yr^{-1}) that streams and rivers likely represent (Beaulieu et al., 2011) is highly uncertain.

Our research goals were to understand and parameterize the influence of hydraulics and streambed morphology on denitrifying microbial community distribution in order to quantify and elucidate specific controls on N_2O production within the HZ. A large-scale flume experiment was conducted where streambed morphology, grain size distribution, flow rate, organic carbon, and nitrate load were constrained and changes in DO, pH, alkalinity, and nitrogen species (NH_3, NO_2, NO_3, N_2O) were monitored regularly. We employed real-time PCR (qPCR) to quantify the distribution of denitrifying functional genes in HZ sediment cores as a measure of denitrifying microorganism abundance. We hypothesized that N_2O production would be controlled by the availability of total nitrogen and dissolved oxygen and the distribution of denitrifying microbial community composition along hyporheic flow paths. We expected to see denitrifying hot spots distributed along hyporheic flow paths with developed anoxic zones, increased NT, and increased abundance of *nirS* and *nosZ*. Additionally, we hypothesized an increase in N_2O production in zones where denitrifying microbial communities have reduced relative abundances of the *nosZ* gene relative to *nirS*. Linear and nonlinear mixed-effects models were used to investigate factors controlling N_2O production within the HZ as a function of total nitrogen (NT) ($NH_3 + NO_2^- + NO_3^-$), relative abundance of *nirS*, *nosZ*, and the ratio of *nosZ* abundance to *nirS* abundance (*nosZ*/*nirS*), and DO.

Methods

Flume Construction and Design

A large (20 m) flume at the Center for Ecohydraulic Research Laboratory at the Idaho Water Center was used for our experiments. The flume was divided into three streams (flumelets), each with an average hyporheic depth of 30 cm. The flumelets were filled with a homogenized sediment mixture comprised of 90% quarry sand (sieved to < 2.4 mm and rinsed to remove fine grains), 10% sand from the upper Boise River serving as the microbial inoculum (sieved to <2.4 mm), and crushed cottonwood leaves (*Populus* sp.), added to a final amount of 0.15% crushed leaves (<5 mm pieces) by dry weight, that served as an endogenous particulate organic carbon source. Sediments were shaped to create bedform dunes 1 m in length, with dunes heights of 3, 6, and 9 cm per flumelet, respectively. Hydraulic conductivity was 0.005 m/s. Holes were drilled into the side of two consecutive dune features along the flow path within each flumelet. Fiber optic DO sensors (PreSens non-invasive oxygen sensor spots (PreSens, Regensburg, Germany) adhered to a fiber optic cable and inserted into a protective stainless steel tube) were installed and connected to the PreSens Fibox via a multiplexer. Additionally Rhizon soil moisture samplers (distributed by Rhizosphere Research Products, Netherlands) were installed to allow for pore water extraction and subsequent geochemical analysis at multiple time points over 16 weeks. Water was pumped (100 gpm) from a large catch basin (50,000 gallon) into a headbox feeding water at an equal rate (33.33 gpm per flumelet) downgradient through all three flumelets and back to the catch basin. At the end of the experiment, the flumelets were slowly drained and sediment cores were removed from the Rhizon ports for microbial community analyses.

Water Sample Collection for N_2O and Water Chemistry Analysis

Water samples for N_2O and water chemistry analyses were collected in prepared and sealed GC vials (preparation described in supplementary methods). Prepared headspace vials were submerged underwater during pore water sampling. A negative pressure was induced within the headspace vials by evacuating each vial with a vacuum pump to ~12 mm Hg. A 27-gauge needle was attached onto the male luer connection of each Rhizon and a pre-evacuated air vial was used to remove and discard water present in the tubing (volume of dead space ~ 0.3 ml, 0.5 mm radius x 36 cm length of tubing). The needle was then immediately placed into the prepared headspace vial and approximately 10 ml of pore water was obtained from each Rhizon port. Sampling occurred downgradient to upgradient. Sample vials remained inverted under water until analyzed by gas chromatography. Surface water samples were also obtained from the catch basin, influent headbox, and within each flumelet.

N_2O Analysis

Pore water N_2O concentrations were determined using a 6890N gas chromatograph (GC) (Agilent Technologies, Santa Clara, CA) equipped with a J&W GS-CarbonPLOT column (length, 30.0 m; diameter, 530.0 μm; film thickness, 3.00 μm) (Agilent Technologies, Santa Clara, CA (model no. 115-3133)) and a ^{63}Ni micro electron capture detector (microECD). The mass of the vials with the sample pore water was recorded and each was placed in the HP 7694 headspace autosampler (Hewlett-Packard, Santa Clara, CA). Concentration of dissolved N_2O was determined following the procedure of Hudson 2004. Briefly, the injection port and oven temperatures were set to 40^{o}C and run time per sample was 3 minutes. The carrier gas was helium for both the

headspace autosampler and GC, make-up gas for the microECD was a mixture of 5% CH_4 in Ar. ECD calibration was performed using standards of (0.0 ppm, prepared just before analysis as described in SI (displacing water with Ar)), 0.1 ppm N_2O, and 1.0 ppm N_2O (Air Liquid America Specialty Gases LLC, Plumsteadville, PA) with no acid addition. After headspace analysis, the remaining water samples were stored at 4^oC until analyzed by a Lachat QuickChem 8500.

Lachat Flow Injection Analysis

Pore water samples were analyzed for nitrate (NO_3^-), nitrite (NO_2^-), and ammonia (NH_3) using the water collected for headspace analysis. Pore water samples from the GC headspace sample vials were transferred into acid washed, pre-weighed sample tubes (PYREX® 16x100 mm culture tube, Corning, NY) with cap (Fisherbrand® TrainerTop™ Safety closures). If the sample volume did not reach at least 12 ml, then milli-Q H_2O (Millipore Corporation, Billerica, MA) was added accordingly and the dilution factor recorded. Samples were stored no more than 48 hours at 4^oC before analysis. An automated ion analyzer (Lachat QuickChem 8500) was employed to quantify nitrate and nitrite (QuickChem Method 10-107-04-1-B), and ammonia (QuickChem Method 10-107-06-1-F) (Lachat Instruments, Loveland, CO).

Microbial Community Analysis

Sediment cores were retrieved from each Rhizon location within the 3, 6, and 9 cm dunes using 310 mm long autoclaved Fisherbrand™ disposable polypropylene spatulas (Thermo Fisher Scientific, Waltham, MA). Samples were placed in sterile 15 mL culture tubes, transported to the lab on dry ice, and then stored at -80^o C until further analysis. Total microbial community DNA was extracted from the sediment cores using the

FastDNA™ SPIN Kit for Soil (MP Biomedical LLC, Solon, OH) following the manufacturer's instructions. The quality of DNA was assessed visually on a 1.5% (wt./vol) agarose gel and quantified using a NanoDrop3300 Fluorospectrometer (Thermo-Scientific, Waltham, MA). Total bacterial densities were quantified by taqman quantitative real-time PCR (qPCR). 16S rRNA gene densities were amplified using forward primer BACT1369F (5'-CGGTGAATACGTTCYCGG-3'), reverse primer PROK1492R (5'-GGWTACCTTGTTACGACTT-3'), and probe TM1389F (5'-6FAM-CTTGTACACACCGCCCGTC-BHQ-3') (Suzuki et al., 2000). PCR run conditions were as described in the supplementary materials. Quantification of the denitrifying genes *nirS*, *nirK*, and *nosZ* was performed using the following primers pairs respectively: nirSCd3aF (5'-AACGYSAAGGARACSGG-3') and nirSR3cd (5'-GASTTCGGRTGSGTCTTSAYGAA-3') (Kandeler et al., 2006), nirK1F (5'-GGMATGGTKCCSTGGCA-3') and nirK5R (5'-GCCTCGATCAGRTTRTGG-3') (Braker et al., 1998), and nosZ2F (5'-CGCRACGGCAASAAGGTSMSSGT-3') and nosZ2R (5'-CAKRTGCAKSGCRTGGCAGAA-3') (Henry et al., 2006). Standards for qPCR reactions were constructed as described in SI.

Statistical Analysis

A linear mixed model (linear and nonlinear mixed-effects models (nlme) package (Pinheiro et al., 2007) in R (Team, 2014)) was used to examine the relationship between N_2O generation within the HZ and environmental parameters such as DO, total nitrogen (NT) (i.e., concentrations of $NH_4^+ + NO_3^- + NO_2^-$), *nirS*, *nosZ*, *nosZ*/*nirS*, dune height (amplitude), and unequal variance by dune. All data was logged and centered about the mean. Spearman rank correlations were calculated for all variables to determine

statistical dependence of any two variables as a means to determine appropriate predictor variables for any given model (Table S1). Any two variables with a correlation coefficient >0.60 were considered auto correlated and not used as predictor variables within the same model. Predictor variable combinations were evaluated by fitting models with maximum likelihood (ML) followed by model selection based on the corrected Akaike information criterion (AICc) (Akaike, 1981). Due to the physical parameters of the flume, mixed models were applied to the data in order to examine the necessity of using spatial covariance structures (spherical, Gaussian, linear, rational, and exponential). Restricted maximum likelihood (REML) was used to calculate the different structures including unequal variance by dune and independence. Residual plots for all top models were validated and residuals were consistent with stochastic error. Final models were fit with REML. The AICcmodavg package in R (Mazerolle, 2012) was employed to compute predicted N_2O values and associated standard errors from predictor variable magnitudes fed into the function for the chosen model.

Results

Development of a Stable Redox Gradient in the HZ

Routine measurements (i.e., 3 events/day) of dissolved oxygen (DO) were taken within the 3, 6, and 9 cm dunes over the course of the experiment in order to track the development of redox conditions within the HZ and determine when conditions reached a quasi-steady state. Distinct redox zones formed within all dunes and included a gradient of oxic (250 µmol/L DO) to completely anoxic (0 µmol/L DO) conditions (Figure 1). Although DO concentrations continued to vary in each dune (3 cm, 6 cm, and 9 cm) between days 77 and 112, the rate of change was slow (e.g., ~ -0.32 µmol/L DO/day

(averaged)) and the DO profiles within each dune remained relatively constant between day 112 (DO was recorded before the last pore water extraction for geochemical analysis prior to sediment extraction) and day 117, 118, and 119 (the last day DO was recorded before sediment extraction for the 9, 6, and 3 cm dune, respectively), indicating a quasi-steady state was established. The pressure distributions at the sediment surface interface were modeled using the computational fluid dynamics program Fluent. The largest pressure gradient was observed in the 9 cm dune where 150 µmol/L DO was recorded as deep as 7 cm within upstream and downstream dunes just before sediment extraction. The flux of oxygenated surface water (i.e., 150 µmol/L DO) into the 6 cm dune was averaged to a depth of 6 cm below the trough. The 3 cm dune had the greatest overall volume of hyporheic area considered anoxic (64% of the ports were within anoxic DO concentrations versus 39% and 23% for the 6 and 9 cm dune, respectively), where 150 µmol/L DO was recorded no deeper than 3 cm below the trough in the upstream and downstream dunes.

Effect of Dune Amplitude on Hyporheic Zone Geochemical Conditions

As surface water (NT ~400 µg N/L) infiltrated the HZ of each flumelet, the concentration distributions of NT varied by dune amplitude (Figure 2). As surface water entered the 3 cm dune, complete removal of NT (<100 µg N/L) occurred within 10 cm of the dune trough as the HZ became anoxic. As surface water entered the 6 cm dune, NT concentrations decreased as pore water fluxed through the upstream dune; however, as surface water penetrated the downstream dune, an increase in NT concentration (hot spot as high as 700 µg N/L) was observed until pore water fluxed into deeper anoxic zones and NT concentrations decreased (<50 µg N/L). The increase in NT concentrations is

also observed within the 9 cm dune as surface water enters the upstream and downstream dunes and is measured as high as 960 µg N/L, whereas the maximum NT concentrations were only 620 and 790 µg N/L for the 3 and 6 cm dunes, respectively. These localized hot spots of increased NT occurred spatially along the gradient from oxic to anoxic with localized NT maxima at zones where DO was between 150 and 180 µmol/L. NT was positively correlated with DO (ρ=0.62, $p < 0.001$, n=168).

N_2O Production

Localized hot spots of N_2O generation developed along the oxic-anoxic transition zone within the 3, 6, and 9 cm dunes as NT concentrations decreased with deeper hyporheic flux (Figure 2). The greatest concentration of N_2O was measured in the 9 cm dune on day 98 (6.21 µg N/L). After 112 days of running the flume, N_2O was measured between 0.04 and 6.04 µg N/L within all amplitudes. Within the 3, 6, and 9 cm dunes respectively, the highest N_2O concentrations recorded within the upstream dune were 1.09, 2.60, and 3.00 µg N/L, whereas the highest concentrations were 0.99, 1.50, and 6.04 µg N/L within the downstream dune on day 112. Concentrations of N_2O were positively correlated with NT (ρ=0.65, $p < 0.001$, n=163). Further, N_2O concentrations were positively correlated with distribution of *nirS* genes (ρ= 0.60, $p < 0.001$, n=163) and *nosZ* genes (ρ= 0.35, $p < 0.001$, n=163), however were negatively correlated to the ratio of *nosZ* gene abundance to *nirS* gene abundance (ρ = -0.28, $p < 0.001$, n=163).

Microbial Distributions Within the Hyporheic Zone

Total bacterial distributions were moderately affected by dune amplitude (Figure 3), whereas streambed morphology uniquely characterized the denitrifying microbial community distributions within each dune according to the hyporheic flux of oxygenated

pore water (Figure 4). Total bacterial distributions were positively and significantly correlated to NT ($\rho = 0.30$; $p<0.001$, n=163), as well as the gene distributions of *nirS* ($\rho = 0.58$), *nirK* ($\rho = 0.60$), and *nosZ* ($\rho = 0.51$). *nirS* and *nosZ* genes were more abundant and widely distributed within the 9 cm dune. *nirS* was significantly and positively correlated with *nirK* ($\rho = 0.56$), *nosZ* ($\rho = 0.65$), N_2O ($\rho = 0.60$), NT ($\rho = 0.35$), and DO ($\rho = 0.44$) ($p<0.001$, n=163). *nosZ* also shared a significant relationship with *nirK* ($\rho = 0.51$) and N_2O ($\rho = 0.35$), and slightly significant correlation with NT ($\rho = 0.24$, $p<0.01$) and DO ($\rho = 0.18$, $p<0.05$). Abundance of *nosZ*/*nirS* increased as pore water moved deeper into the HZ as well as within locations spatially located near upwelling flows where pore water mixes with the surface water column (Figure 5). A negative relationship was found between *nosZ*/*nirS* and N_2O ($\rho = -0.28$, $p=0.007$), NT ($\rho = -0.14$, $p<0.01$), and DO ($\rho = -0.33$, $p<0.001$). *nirK* had minimal significant correlation with N_2O ($\rho = 0.17$, $p<0.05$, n=163) and NT ($\rho = 0.15$, $p<0.05$, n=163) and no significance with DO. It also had a lower relative magnitude than *nirS* and was therefore not considered in statistical modeling efforts.

Spatial Statistical Modeling

We employed statistical evaluations of biogeochemical and hydrological parameters to examine factors influencing N_2O production with the HZ. A statistical workflow, including multiple rounds of AICc model selection, was applied to evaluate the best predictor variable combination for N_2O. Initial model selection included evaluating all combinations of modeling terms NT, DO, *nirS*, and *nosZ*/*nirS* as well as interactions between terms. *nosZ* was not included as a predictor variable for N_2O because its presence is inherently correlated with that of *nirS* ($\rho_{XY} = 0.65$). Therefore, the

relative abundance of *nosZ* to *nirS* (*nosZ*/*nirS*) was used as a predictor variable in order to evaluate the overall distribution of denitrifying microbial community gene abundance and N_2O production, and to account for the relative distribution of these two functional genes as a factor. Top models were further evaluated with dune height, unequal variance between dune structures, as well as their fixed effect interaction term.

The best predictor variable combination for N_2O included NT, DO, *nirS*, height (dune amplitude), dune as an ordered factor, and interaction terms between NT and *nirS*, NT and DO, as well as between height and dune (AICc 67.21 with maximum likelihood) (Table 1). DO, as an independent variable alone, was found unsuitable to predict N_2O, receiving an Akaike weight of 189.30 (model B_5) (Table S2). DO and NT shared a correlation coefficient of 0.60 and were considered as coexisting predictor variables in testing our hypothesis that N_2O production within the HZ is a function of microbial gene distribution, total nitrogen, and DO availability. Predictive power of the model increased when DO was combined with NT as Akaike weights decreased 42 units (147.30) (model D_1) (Table S2) and therefore model selection efforts only considered DO as a possible variable when NT was also considered. The predictive capacity of NT and DO for N_2O was further improved once an interaction term between NT and DO was included (144.27) (model D_2) (Table S2). A significant improvement to the predictive capacity occurred once *nirS* and the interactive term between NT and *nirS* were added to models D_1 and D_2, decreasing the Akaike weights by at least 39 units (105.26 for model A_14_B and 105.34 for model A_15) (Table S2). Model A_15 may be a more parsimonious model, however further evaluation of predictive parameters including height (dune amplitude) and/or dune as an ordered factor, as well as their interaction term

significantly improved the predictive capacity of model A_14_B as the Akaike weight decreased from 105.26 to 67.21 (model A_14_B_dune_height_C) (Table S3). An unequal variance structure was applied to the final model, as confirmed by AICc (Table S4) and was evaluated with REML (variance by dune: dune 1= 1.00, dune 2 = 1.40).

Discussion

Streams and rivers are hydraulically connected to terrestrial ecosystems and consequently are subjected to increased loads of Nr that originate from terrestrial application of nitrogenous fertilizers. The HZ may provide an ecologically important sink for Nr because it (1) contains sediments with large amounts of surface area on which microbial communities can develop, (2) continually receives solutes through surface and groundwater sources, and (3) has a high surface area to volume ratio, which can provide extended contact (i.e., reaction times) between solutes and microbial communities, allowing for important reactions, such as nitrification and denitrification, to take place (Harvey et al., 2013; Merill and Tonjes, 2014; Boano et al., 2010; Winter, 1998). N_2O is an intermediate in these reactions; therefore, establishing the extent to which streams and rivers contribute to the global emissions of this potent greenhouse gas is important for improving our ability to predict the role of fluvial systems in models of greenhouse gas production.

Within the construct of our large-scale flume experiment, we were able to unravel the complexities of a natural system and delineate specific controls on N_2O generation within the HZ. N_2O generation was best characterized by geochemical, biological, and geomorphological variables as well as interactions among them. AICc model selection supported our hypothesis that denitrifying hot spots (i.e., locations of elevated N_2O

generation) would occur along flow paths with developed anoxic zones, increased NT and increased abundance of denitrifying genes, *nirS* and *nosZ*. Predictor variable input values were centered about the mean prior to statistical evaluation. This facilitated the interpretation of the results and provided a way to clearly evaluate the relationships among variables and interaction terms. Table 2 provides the 10th, 30th, 70th, and 90th percentiles and mean values within our data, as well as the corresponding mean-centered modeling data input. We reference these values in our discussion to illustrate how the estimates for each model term can be dependent on the interactions among predictor variables.

Geochemical Controls on N_2O Production

The statistically significant interaction between NT and DO affected the relative magnitude of the coefficient for the relationship between N_2O and NT (Table 1) and exposed NT as a strong determinant for N_2O when DO is at or below the mean concentration. The coefficient of any modeling parameter represents the mean change in the response variable to a one-unit change in the predictor variable while other modeling parameters are held constant. The input value for one interaction variable (e.g., DO) can be distributed into the coefficient of the interaction term (NT*DO). This newly weighted coefficient can then be distributed throughout like terms within the model, thereby adjusting the overall mean change in the response variable (i.e., N_2O), to the newly reduced predictor variable, in this case NT. For example, if the mean concentration for DO is considered (31 μmol/L, as centered data this value is set to = 0), and all other parameters are held constant, the interaction term (NT*DO) becomes 0 and the coefficient for the relationship between N_2O and NT is 0.44. When DO levels are high

and conditions oxic (e.g., at the 90th percentile DO concentration = 217 μmol/L, as centered data = 0.60), the overall mean change of N_2O to a one-unit increase in NT is reduced as the coefficient for the relationship between N_2O and NT decreases to 0.18. Further, as NT enters a region within the HZ with decreased DO, suboxic (-0.22, 6.3 μmol/L) or anoxic (-0.30, 0 μmol/L), the mean change of N_2O to a one-unit change in NT increases to 0.54 and 0.57, respectively. This was not unexpected as the primary metabolism by which N_2O is being produced in our system (i.e., denitrification) is anaerobic.

The effect of the interaction between NT and DO to denitrification (N_2O generation) is coupled to the availability of organic carbon. Others have made a similar observation in a natural system where NO_3^- removal efficiency via denitrification increased not as a result of increased NO_3^- alone, but as ecosystem respiration rates increased (Mulholland et al., 2008b). They attribute this to a decrease in DO concentration and subsequent increase in the need for alternative electron acceptors like NO_3^- and other intermediates of denitrification. Denitrifiers are equipped with transcriptional and post-transcriptional controls that block the synthesis of denitrifying enzymes when in direct contact with O_2 (Bakken et al., 2012; van Spanning et al., 2007). However, these control mechanisms differ for each reductase and denitrifying organism (Otte et al., 1996; Jones et al., 2013). For example, the enzyme that reduces N_2O to N_2 is more sensitive to oxygen than other reductases (Otte et al., 1996; Ligi et al., 2013; Wrage et al., 2001) and its expression appears to lag behind expression of the other genes associated with denitrification when an organism is transferred from aerobic to anaerobic conditions (Bakken and Dörsch, 2007). The system must have enough labile organic

carbon to induce respiration, deplete DO to a concentration suitable for synthesis of all denitrifying enzymes, and sustain complete reduction of NO_3^- to N_2 (e.g., available as an electron donor).

Microbial Community Influence on N_2O Production in the HZ

In addition to the geochemical controls on N_2O production, our model selection indicated that the population density of denitrifying organisms influenced N_2O concentrations in the HZ. More specifically, AICc based model selection significantly supported the addition of *nirS* and its interaction term between *nirS* and NT (*nirS**NT) to improve prediction of N_2O generation. *nirS* and NT both shared a highly significant positive relationship with N_2O. Therefore, when NT was above the mean concentration, and when all other parameters were held constant, the interaction term increased the overall magnitude of the coefficient between N_2O and *nirS*. For example, at 70^{th} and 90^{th} percentile NT concentrations (200 µg N/L (0.30) and 630 µg N/L (0.80)), the magnitude of the coefficient for N_2O and *nirS* is 0.42 and 0.58, respectively. Further, *nirS* abundance only explained N_2O concentration profiles when the magnitude of abundance was above the mean abundance of our data (i.e., >5.01E+06 copy #/gram dry sediment). This is discernible upon consideration of the centered mean *nirS* abundance (0), which cancels out the predictive weight of *nirS* as well as the interaction between *nirS* and NT. At any abundance below the mean, where the *nirS* term would have a negative magnitude (i.e., 30^{th} percentile (-0.30, 2.51E+06 copy #/gram dry sediment)), a reduction in N_2O generation would be predicted.

The presence of *nirS* did not always result in an increase in predicted N_2O generation. Denitrifying genes are common within environmental samples and detecting

the presence of these genes does not indicate that the genes are being expressed (Wallenstein et al., 2006; Philippot et al., 2001). An increased abundance of bacteria containing *nirS* can only suggest that localized areas have the ability to undergo denitrification if conditions are favorable. At the same time, it is possible that localized areas that have favorable conditions for denitrification will select for denitrifiers and result in an increased abundance of the *nirS* gene. Localized areas with a relative low abundance of *nirS*, may still undergo denitrification, however its relative significance to overall N_2O generation is minimal.

Although not found to be a suitable predictor variable for N_2O generation, there was a significant negative relationship between N_2O and the *nosZ*/*nirS* ratio (Table S5). This provides some evidence that N_2O concentrations decrease in local areas where there is increased relative abundance of *nosZ*. In addition, as oxygen is depleted, induction of the reductases is stepwise and complete expression of the genes necessary for complete denitrification is further dependent on the concentration of nitrogen oxide intermediates (Otte et al., 1996; Körner and Zumft, 1989; Baumann et al., 1996; Kučera et al., 1986; WAKI et al., 1980). Where there is a transient accumulation of N_2O in our system, with an increased relative abundance of *nirS* and DO concentrations above 31 μmol/L, we would expect to see increased levels of transcribed *nirS* relative to transcribed *nosZ*.

To our knowledge, this is the first application of spatial statistical methods incorporating denitrifying functional gene distribution to predict N_2O generation within the HZ. Our modeling efforts describe a highly significant positive relationship between N_2O generation and *nirS* gene abundance. Others have described a positive relationship between denitrification and functional genes; however, few have found this relationship

to be significant (Harvey et al., 2013; Dong et al., 2009; Barrett et al., 2013). A study investigating denitrification activity found that a greater amount of available NO_3^- produced greater induction and longer expression of *nirS* (Saleh-Lakha et al., 2009). Although we did not measure expression of functional genes, this could support the significant correlation we found between the interaction of NT and *nirS* gene abundance and N_2O generation. Including microbial denitrifier abundance, such as *nirS*, in models predicting N_2O from fluvial systems could improve parameterization of denitrification rates and improve our ability to predict N_2O from these systems.

Geomorphological Influence on N_2O Production

Hydraulic conditions induced by geomorphological features influenced biological transformation of NT and N_2O generation within the HZ. AICc model selection supported the addition of dune height (amplitude) and dune as an ordered factor allowing for the interrogation of head variation on N_2O distribution with the HZ. The interaction between dune height and dune as an ordered factor was highly significant, therefore the inclusion of height as a variable, although not significant, was required. The significance of dune is likely an artifact of the upstream and downstream dunes not being identical replicates of each other. Slight variations in the homogeneity of sediment and organic carbon distributions at the time of flume construction made it challenging to construct two identical dunes in which to perform our experiment. Furthermore, over the 112 days of running the flume, natural scouring may have shifted the precise elevation of dune morphologies, inducing slightly different hyporheic exchange within the upstream and downstream dunes. This was statistically accounted for by applying the nlme package, allowing for errors to be correlated and have unequal variances.

Dune was set as an ordered factor denoting the upstream dunes as 0 and downstream dunes as 1. With this defined, the effect of dune height on N_2O generation can be explored using the middle position (0.5) within the factors as the value for dune. When 0.5 is used as the magnitude for dune in the interaction term, the coefficient for N_2O and dune height is 0.04. This coefficient may appear nominal, however when multiplied throughout each dune height, 3, 6 or 9 cm, the weighted influence of hydraulics becomes evident (i.e., weighted influence of 0.12, 0.24, and 0.36 for the 3, 6, and 9 cm dunes, respectively). Dune as an ordered factor was also highly significant and when the 0.5 "position" is considered, the weighted influence of dune for N_2O generation is -0.29. This weighted value combined with the weighted value of dune height along with the interaction term provided an overall weighted hydraulic influence of -0.17, -0.05, 0.07 for the 3, 6, and 9 cm dunes, respectively on N_2O generation.

Mass exchange between the surface water and HZ is driven by pressure variations over bed forms (Elliott and Brooks, 1997; Marion et al., 2002; Packman et al., 2004). Hydraulic gradient distributions can also be a governing factor over nitrogen transformations within the HZ as it regulates the rate at which NT, DO, and dissolved organic carbon (DOC) are supplied (Baker et al., 2000; Zarnetske et al., 2011a; Triska et al., 1993; Harvey et al., 2013). We ascribe the hydraulic control on N_2O generation to the magnitude of oxic water flux into the HZ as a result of dune height and corresponding pressure gradient distribution. In our system, this differential in O_2 rich surface water flux into the HZ resulted in a larger oxic zone in the 9 cm dune relative to the 6 and 3 cm dune heights. This deeper flux of oxygenated water into the 9 cm dune ultimately led to increased N_2O generation. As oxygenated water infiltrated with downwelling flows,

aerobic decomposition of organic matter was stimulated, and NH_3 was released and subsequently oxidized to NO_3^- via nitrification, increasing NT. Further, the increased flux of oxygenated surface water resulted a greater volume characterized as an oxic-anoxic transition zone, within which incomplete denitrification may have dominated given that *nosZ* is more sensitive to DO concentrations than *nirS*.

Conclusion

N_2O generation within our system was highly dependent on the availability of NT when DO was at or below 31 μmol/L. The addition of denitrifying gene abundance, *nirS*, as a modeling parameter significantly improved the quality of our model. Our statistical model also emphasized the role of streambed morphology on N_2O generation, which is likely due to its control over the delivery of electron acceptors such as DO, NO_3^-, and NO_2^-, as well as electron donors such as carbon and NH_3 to hyporheic microbial communities. Other research suggests that an increase in the quantity and quality of carbon can promote NO_3^- removal efficiency, which is also controlled by hydraulic dynamics (Arango et al., 2007; Zarnetske et al., 2011b). As global population increases, increased anthropogenic Nr contributions to fluvial systems are inevitable. In order to mitigate these systems without increasing N_2O generation, it is important to enrich our understanding regarding the connection between the spatio-temporal changes induced by streambed morphology and biogeochemical parameters such as NT, DO, labile DOC, and denitrifying microbial community abundance.

References

Akaike, H. (1981) 'Likelihood of a model and information criteria', *Journal of econometrics,* 16(1), pp. 3-14.

Almeida, J., Reis, M. and Carrondo, M. (1997) 'A unifying kinetic model of denitrification', *Journal of theoretical biology,* 186(2), pp. 241-249.

Arango, C. P., Tank, J. L., Schaller, J. L., Royer, T. V., Bernot, M. J. and David, M. B. (2007) 'Benthic organic carbon influences denitrification in streams with high nitrate concentration', *Freshwater Biology,* 52(7), pp. 1210-1222.

Baker, M. A., Valett, H. M. and Dahm, C. N. (2000) 'Organic carbon supply and metabolism in a shallow groundwater ecosystem', *Ecology,* 81(11), pp. 3133-3148.

Bakken, L. and Dörsch, P. (2007) 'Nitrous oxide emissions and global changes: modelling approaches', *Biology of the nitrogen cycle,* pp. 382-395.

Bakken, L. R., Bergaust, L., Liu, B. and Frostegård, Å. (2012) 'Regulation of denitrification at the cellular level: a clue to the understanding of N2O emissions from soils', *Philosophical Transactions of the Royal Society B: Biological Sciences,* 367(1593), pp. 1226-1234.

Barrett, M., Jahangir, M. M., Lee, C., Smith, C. J., Bhreathnach, N., Collins, G., Richards, K. G. and O'Flaherty, V. (2013) 'Abundance of denitrification genes under different peizometer depths in four Irish agricultural groundwater sites', *Environmental Science and Pollution Research,* 20(9), pp. 6646-6657.

Baumann, B., Snozzi, M., Zehnder, A. and Van Der Meer, J. R. (1996) 'Dynamics of denitrification activity of Paracoccus denitrificans in continuous culture during aerobic-anaerobic changes', *Journal of Bacteriology,* 178(15), pp. 4367-4374.

Beaulieu, J. J., Tank, J. L., Hamilton, S. K., Wollheim, W. M., Hall, R. O., Mulholland, P. J., Peterson, B. J., Ashkenas, L. R., Cooper, L. W. and Dahm, C. N. (2011) 'Nitrous oxide emission from denitrification in stream and river networks', *Proceedings of the National Academy of Sciences,* 108(1), pp. 214-219.

Betlach, M. R. and Tiedje, J. M. (1981) 'Kinetic explanation for accumulation of nitrite, nitric oxide, and nitrous oxide during bacterial denitrification', *Applied and Environmental Microbiology,* 42(6), pp. 1074-1084.

Boano, F., Demaria, A., Revelli, R. and Ridolfi, L. (2010) 'Biogeochemical zonation due to intrameander hyporheic flow', *Water resources research,* 46(2).

Böhlke, J. K., Antweiler, R. C., Harvey, J. W., Laursen, A. E., Smith, L. K., Smith, R. L. and Voytek, M. A. (2009) 'Multi-scale measurements and modeling of denitrification in streams with varying flow and nitrate concentration in the upper Mississippi River basin, USA', *Biogeochemistry,* 93(1-2), pp. 117-141.

Bothe, H., Ferguson, S. and Newton, W. E. (2006) *Biology of the nitrogen cycle.* Elsevier.

Boulton, A. J., Findlay, S., Marmonier, P., Stanley, E. H. and Valett, H. M. (1998) 'The functional significance of the hyporheic zone in streams and rivers', *Annual Review of Ecology and Systematics*, pp. 59-81.

Braker, G., Fesefeldt, A. and Witzel, K.-P. (1998) 'Development of PCR primer systems for amplification of nitrite reductase genes (nirK and nirS) to detect denitrifying bacteria in environmental samples', *Applied and Environmental Microbiology*, 64(10), pp. 3769-3775.

Buffington, J. M. and Tonina, D. (2009) 'Hyporheic exchange in mountain rivers II: Effects of channel morphology on mechanics, scales, and rates of exchange', *Geography Compass*, 3(3), pp. 1038-1062.

Carpenter, S. R., Caraco, N. F., Correll, D. L., Howarth, R. W., Sharpley, A. N. and Smith, V. H. (1998) 'Nonpoint pollution of surface waters with phosphorus and nitrogen', *Ecological applications*, 8(3), pp. 559-568.

Chapelle, F. H., McMahon, P. B., Dubrovsky, N. M., Fujii, R. F., Oaksford, E. T. and Vroblesky, D. A. (1995) 'Deducing the distribution of terminal electron-accepting processes in hydrologically diverse groundwater systems', *Water Resources Research*, 31(2), pp. 359-371.

Coyne, M. S. and Tiedje, J. M. (1990) 'Induction of denitrifying enzymes in oxygen-limited Achromobacter cycloclastes continuous culture', *FEMS Microbiology Letters*, 73(3), pp. 263-270.

Čuhel, J., Šimek, M., Laughlin, R. J., Bru, D., Chèneby, D., Watson, C. J. and Philippot, L. (2010) 'Insights into the effect of soil pH on N2O and N2 emissions and denitrifier community size and activity', *Applied and environmental microbiology*, 76(6), pp. 1870-1878.

Davies, K. J., Lloyd, D. and Boddy, L. (1989) 'The effect of oxygen on denitrification in Paracoccus denitrificans and Pseudomonas aeruginosa', *Microbiology*, 135(9), pp. 2445-2451.

Dong, L. F., Smith, C. J., Papaspyrou, S., Stott, A., Osborn, A. M. and Nedwell, D. B. (2009) 'Changes in benthic denitrification, nitrate ammonification, and anammox process rates and nitrate and nitrite reductase gene abundances along an estuarine nutrient gradient (the Colne Estuary, United Kingdom)', *Applied and environmental microbiology*, 75(10), pp. 3171-3179.

Elliott, A. H. and Brooks, N. H. (1997) 'Transfer of nonsorbing solutes to a streambed with bed forms: Laboratory experiments', *Water Resources Research*, 33(1), pp. 137-151.

Erisman, J. W., Sutton, M. A., Galloway, J., Klimont, Z. and Winiwarter, W. (2008) 'How a century of ammonia synthesis changed the world', *Nature Geoscience*, 1(10), pp. 636-639.

Forster, P., Ramaswamy, V., Artaxo, P., Berntsen, T., Betts, R., Fahey, D. W., Haywood, J., Lean, J., Lowe, D. C. and Myhre, G. (2007) 'Changes in atmospheric constituents and in radiative forcing. Chapter 2', *Climate Change 2007. The Physical Science Basis*.

Galloway, J. N., Townsend, A. R., Erisman, J. W., Bekunda, M., Cai, Z., Freney, J. R., Martinelli, L. A., Seitzinger, S. P. and Sutton, M. A. (2008) 'Transformation of the nitrogen cycle: recent trends, questions, and potential solutions', *Science*, 320(5878), pp. 889-892.

Harvey, J. W., Böhlke, J. K., Voytek, M. A., Scott, D. and Tobias, C. R. (2013) 'Hyporheic zone denitrification: Controls on effective reaction depth and contribution to whole‐stream mass balance', *Water Resources Research*, 49(10), pp. 6298-6316.

Henry, S., Bru, D., Stres, B., Hallet, S. and Philippot, L. (2006) 'Quantitative detection of the nosZ gene, encoding nitrous oxide reductase, and comparison of the abundances of 16S rRNA, narG, nirK, and nosZ genes in soils', *Applied and Environmental Microbiology*, 72(8), pp. 5181-5189.

Holtan-Hartwig, L., Dörsch, P. and Bakken, L. R. (2000) 'Comparison of denitrifying communities in organic soils: kinetics of NO− 3 and N 2 O reduction', *Soil Biology and Biochemistry*, 32(6), pp. 833-843.

Hudson, F. (2004) 'Sample Preparation and Calculations for Dissolved Gas Analysis in Water Samples Using a GC Headspace Equilibration Technique', *Method RSKSOP-175, US Environmental Protection Agency (EPA) Region*, 1.

Ingersoll, T. L. and Baker, L. A. (1998) 'Nitratfe removal in wetland microcosms', *Water research*, 32(3), pp. 677-684.

Jones, C. M., Graf, D. R., Bru, D., Philippot, L. and Hallin, S. (2013) 'The unaccounted yet abundant nitrous oxide-reducing microbial community: a potential nitrous oxide sink', *The ISME journal*, 7(2), pp. 417-426.

Jones, C. M., Stres, B., Rosenquist, M. and Hallin, S. (2008) 'Phylogenetic analysis of nitrite, nitric oxide, and nitrous oxide respiratory enzymes reveal a complex evolutionary history for denitrification', *Molecular biology and evolution*, 25(9), pp. 1955-1966.

Kandeler, E., Deiglmayr, K., Tscherko, D., Bru, D. and Philippot, L. (2006) 'Abundance of narG, nirS, nirK, and nosZ genes of denitrifying bacteria during primary successions of a glacier foreland', *Applied and Environmental Microbiology*, 72(9), pp. 5957-5962.

Kellman, L. and Hillaire-Marcel, C. (1998) 'Nitrate cycling in streams: using natural abundances of NO3--δ15N to measure in-situ denitrification', *Biogeochemistry*, 43(3), pp. 273-292.

Kjellin, J., Hallin, S. and Wörman, A. (2007) 'Spatial variations in denitrification activity in wetland sediments explained by hydrology and denitrifying community structure', *Water Research*, 41(20), pp. 4710-4720.

Körner, H. and Zumft, W. G. (1989) 'Expression of denitrification enzymes in response to the dissolved oxygen level and respiratory substrate in continuous culture of Pseudomonas stutzeri', *Applied and Environmental Microbiology*, 55(7), pp. 1670-1676.

Kozub, D. and Liehr, S. (1999) 'Assessing denitrification rate limiting factors in a constructed wetland receiving landfill leachate', *Water Science and technology,* 40(3), pp. 75-82.

Krause, S., Hannah, D., Fleckenstein, J., Heppell, C., Kaeser, D., Pickup, R., Pinay, G., Robertson, A. and Wood, P. (2011) 'Interdisciplinary perspectives on processes in the hyporheic zone', *Ecohydrology,* 4(4), pp. 481-499.

Kučera, I., Matyášek, R., Dvořáková, J. and Dadák, V. (1986) 'Anaerobic adaptation ofParacoccus denitrificans: Sequential formation of denitrification pathway and changes in activity of 5-aminolevulinate synthase and catalase', *Current Microbiology,* 13(2), pp. 107-110.

Kuňák, M., Kučera, I. and Van Spanning, R. J. (2004) 'Nitric oxide oscillations in Paracoccus denitrificans: the effects of environmental factors and of segregating nitrite reductase and nitric oxide reductase into separate cells', *Archives of biochemistry and biophysics,* 429(2), pp. 237-243.

Laursen, A. E. and Seitzinger, S. P. (2004) 'Diurnal patterns of denitrification, oxygen consumption and nitrous oxide production in rivers measured at the whole‐reach scale', *Freshwater Biology,* 49(11), pp. 1448-1458.

Ligi, T., Truu, M., Truu, J., Nõlvak, H., Kaasik, A., Mitsch, W. J. and Mander, Ü. (2014) 'Effects of soil chemical characteristics and water regime on denitrification genes (nirS, nirK, and nosZ) abundances in a created riverine wetland complex', *Ecological Engineering* 72, pp.47-55.

Lin, Y.-F., Jing, S.-R., Wang, T.-W. and Lee, D.-Y. (2002) 'Effects of macrophytes and external carbon sources on nitrate removal from groundwater in constructed wetlands', *Environmental pollution,* 119(3), pp. 413-420.

Liu, B., Frostegård, Å. and Bakken, L. R. (2014) 'Impaired reduction of N2O to N2 in acid soils is due to a posttranscriptional interference with the expression of nosZ', *mBio,* 5(3), pp. e01383-14.

Malard, F., Tockner, K., DOLE-OLIVIER, M. J. and Ward, J. (2002) 'A landscape perspective of surface–subsurface hydrological exchanges in river corridors', *Freshwater Biology,* 47(4), pp. 621-640.

Marion, A., Bellinello, M., Guymer, I. and Packman, A. (2002) 'Effect of bed form geometry on the penetration of nonreactive solutes into a streambed', *Water Resources Research,* 38(10), pp. 27-1-27-12.

Mazerolle, M. 2012. AICcmodavg: model selection and multimodel inference based on (Q) AIC (c). R package version 1.26. R Project for Statistical Computing Vienna, Austria.

Merill, L. and Tonjes, D. J. (2014) 'A review of the hyporheic zone, stream restoration, and means to enhance denitrification', *Critical Reviews in Environmental Science and Technology,* 44(21), pp. 2337-2379.

Morley, N., Baggs, E. M., Dörsch, P. and Bakken, L. (2008) 'Production of NO, N2O and N2 by extracted soil bacteria, regulation by NO2− and O2 concentrations', *FEMS microbiology ecology,* 65(1), pp. 102-112.

Morrice, J. A., Dahm, C. N., Valett, H. M., Unnikrishna, P. V. and Campana, M. E. (2000) 'Terminal electron accepting processes in the alluvial sediments of a headwater stream', *Journal of the North American Benthological Society,* 19(4), pp. 593-608.

Mulholland, P. J., Helton, A. M., Poole, G. C., Hall, R. O., Hamilton, S. K., Peterson, B. J., Tank, J. L., Ashkenas, L. R., Cooper, L. W. and Dahm, C. N. (2008b) 'Stream denitrification across biomes and its response to anthropogenic nitrate loading', *Nature,* 452(7184), pp. 202-205.

Nielsen, L. P., Christensen, P. B., Revsbech, N. P. and Sørensen, J. (1990) 'Denitrification and oxygen respiration in biofilms studied with a microsensor for nitrous oxide and oxygen', *Microbial Ecology,* 19(1), pp. 63-72.

Otte, S., Grobben, N. G., Robertson, L. A., Jetten, M. and Kuenen, J. G. (1996) 'Nitrous oxide production by Alcaligenes faecalis under transient and dynamic aerobic and anaerobic conditions', *Applied and environmental microbiology,* 62(7), pp. 2421-2426.

Packman, A. I., Salehin, M. and Zaramella, M. (2004) 'Hyporheic exchange with gravel beds: basic hydrodynamic interactions and bedform-induced advective flows', *Journal of Hydraulic Engineering,* 130(7), pp. 647-656.

Philippot, L., Mirleau, P., Mazurier, S., Siblot, S., Hartmann, A., Lemanceau, P. and Germon, J. (2001) 'Characterization and transcriptional analysis of Pseudomonas fluorescens denitrifying clusters containing the nar, nir, nor and nos genes', *Biochimica et Biophysica Acta (BBA)-Gene Structure and Expression,* 1517(3), pp. 436-440.

Pinheiro, J., Bates, D., DebRoy, S. and Sarkar, D. (2007) 'Linear and nonlinear mixed effects models', *R package version,* 3, pp. 57.

Ravishankara, A., Daniel, J. S. and Portmann, R. W. (2009) 'Nitrous oxide (N2O): the dominant ozone-depleting substance emitted in the 21st century', *science,* 326(5949), pp. 123-125.

Richardson, D. J., van Spanning, R. and Ferguson, S. J. (2007) 'The prokaryotic nitrate reductases', *Biology of the Nitrogen Cycle,* pp. 21-35.

Sakita, S. and Kusuda, T. (2000) 'Modeling and simulation with microsites on vertical concentrationprofiles in sediments of aquatic zones', *Water Science & Technology,* 42(3-4), pp. 409-415.

Saleh-Lakha, S., Shannon, K. E., Henderson, S. L., Zebarth, B. J., Burton, D. L., Goyer, C. and Trevors, J. T. (2009) 'Effect of nitrate and acetylene on nirS, cnorB, and nosZ expression and denitrification activity in Pseudomonas mandelii', *Applied and environmental microbiology,* 75(15), pp. 5082-5087.

Schaller, J. L., Royer, T. V., David, M. B. and Tank, J. L. (2004) 'Denitrification associated with plants and sediments in an agricultural stream', *Journal of the North American Benthological Society*, 23(4), pp. 667-676.

Seitzinger, S. P., Kroeze, C. and Styles, R. V. (2000) 'Global distribution of N 2 O emissions from aquatic systems: natural emissions and anthropogenic effects', *Chemosphere-Global Change Science*, 2(3), pp. 267-279.

Šimek, M. and Cooper, J. (2002) 'The influence of soil pH on denitrification: progress towards the understanding of this interaction over the last 50 years', *European Journal of Soil Science*, 53(3), pp. 345-354.

Stanford, J. A. and Ward, J. (1993) 'An ecosystem perspective of alluvial rivers: connectivity and the hyporheic corridor', *Journal of the North American Benthological Society*, pp. 48-60.

Sutton, M. A., Oenema, O., Erisman, J. W., Leip, A., van Grinsven, H. and Winiwarter, W. (2011) 'Too much of a good thing', *Nature*, 472(7342), pp. 159-161.

Suzuki, M. T., Taylor, L. T. and DeLong, E. F. (2000) 'Quantitative analysis of small-subunit rRNA genes in mixed microbial populations via 5′-nuclease assays', *Applied and Environmental Microbiology*, 66(11), pp. 4605-4614.

Sørensen, J., Jørgensen, B. B. and Revsbech, N. P. (1979) 'A comparison of oxygen, nitrate, and sulfate respiration in coastal marine sediments', *Microbial Ecology*, 5(2), pp. 105-115.

R Development Core Team (2014), R: A Language and Environment for Statistical Computing. Vienna, Austria: the R Foundation for Statistical Computing. ISBN 3-900051-07-0. Available online at http://www.R-project.org/.

Tonina, D. and Buffington, J. M. (2009) 'Hyporheic exchange in mountain rivers I: Mechanics and environmental effects', *Geography Compass*, 3(3), pp. 1063-1086.

Triska, F. J., Duff, J. H. and Avanzino, R. J. (1993) 'Patterns of hydrological exchange and nutrient transformation in the hyporheic zone of a gravel‐bottom stream: examining terrestrial—aquatic linkages', *Freshwater Biology*, 29(2), pp. 259-274.

Triska, F. J., Kennedy, V. C., Avanzino, R. J., Zellweger, G. W. and Bencala, K. E. (1989) 'Retention and transport of nutrients in a third-order stream: channel processes', *Ecology*, pp. 1877-1892.

van Spanning, R. J., Richardson, D. J. and Ferguson, S. J. (2007) 'Introduction to the biochemistry and molecular biology of denitrification', *Biology of the nitrogen cycle*, pp. 3-20.

WAKI, T., MURAYAMA, K.-I., KAWATO, Y. and ICHIKAWA, K. (1980) 'Transient Characteristics of Paracoccus denitrificans with Changes between Aerobic and Anaerobi Conditions', *Journal of fermentation technology*, 58(3), pp. 243-249.

Wallenstein, M. D., Myrold, D. D., Firestone, M. and Voytek, M. (2006) 'Environmental controls on denitrifying communities and denitrification rates: insights from molecular methods', *Ecological applications*, 16(6), pp. 2143-2152.

Winter, T. C. (1998) Ground water and surface water: a single resource. DIANE Publishing Inc.

Wood, D. W., Setubal, J. C., Kaul, R., Monks, D. E., Kitajima, J. P., Okura, V. K., Zhou, Y., Chen, L., Wood, G. E. and Almeida, N. F. (2001) 'The genome of the natural genetic engineer Agrobacterium tumefaciens C58', *Science*, 294(5550), pp. 2317-2323.

Wrage, N., Velthof, G., Van Beusichem, M. and Oenema, O. (2001) 'Role of nitrifier denitrification in the production of nitrous oxide', *Soil Biology and Biochemistry*, 33(12), pp. 1723-1732.

Zarnetske, J. P., Haggerty, R., Wondzell, S. M. and Baker, M. A. (2011a) 'Dynamics of nitrate production and removal as a function of residence time in the hyporheic zone', *Journal of Geophysical Research: Biogeosciences (2005–2012)*, 116(G1).

Zarnetske, J. P., Haggerty, R., Wondzell, S. M. and Baker, M. A. (2011b) 'Labile dissolved organic carbon supply limits hyporheic denitrification', *Journal of Geophysical Research: Biogeosciences (2005–2012)*, 116(G4).

Zumft, W. G. (1997) 'Cell biology and molecular basis of denitrification', *Microbiology and molecular biology reviews*, 61(4), pp. 533-616.

Zumft, W. G., Döhler, K. and Körner, H. (1985) 'Isolation and characterization of transposon Tn5-induced mutants of Pseudomonas perfectomarina defective in nitrous oxide respiration', *Journal of bacteriology*, 163(3), pp. 918-924.

Tables

Table 1: Analysis of Variance for the Top Model (response variable: N_2O). The top model was confirmed through statistical evaluation (using the linear and nonlinear mixed effects models (nlme) package in R) of all possible modeling parameters using maximum likelihood and multiple rounds of AICc model selection. An unequal variance structure by dune (variance by dune: dune 1= 1.00 and dune 2= 1.40) was confirmed via AICc model selection and applied to the final model. The final model was evaluated with restricted maximum likelihood.

Model Parameter	Coefficient	Standard Error	95% Confidence Intervals	p-value
Intercept	0.05	0.08	(-0.11, 0.20)	0.561
NT	0.44	0.05	(0.34, 0.54)	0.000
DO	-0.05	0.10	(-0.24, 0.15)	0.621
nirS	0.33	0.05	(0.23, 0.43)	0.000
dune	-0.58	0.12	(-0.82, -0.34)	0.000
height	0.01	0.01	(-0.01, 0.03)	0.287
NT*nirS	0.31	0.09	(0.13, 0.50)	0.001
NT*DO	-0.44	0.16	(-0.75, -0.12)	0.006
dune*height	0.06	0.02	(0.03, 0.10)	0.001

Table 2: Modeling Parameter Inputs. All variables (response and predictor variables) were logged and centered about the mean prior to statistical evaluation. Here, the 10th, 30th, 70th, and 90th percentiles and mean values within our data for the predictor variables chosen as the top modeling parameters are provided along with their corresponding centered modeling data input to facilitate interpretation of modeling results.

	NT (data input for R)	NT (µg N/L)	DO (data input for R)	DO (µmol/L)	*nirS* (data input for R)	*nirS* (copy #/gram dry sediment)
10th percentile	-0.70	20	-0.30	0	-0.60	1.26E+06
30th percentile	-0.30	50	-0.22	6.3	-0.30	2.51E+06
mean	0.00	100	0.00	31	0.00	5.01E+06
70th percentile	0.30	200	0.18	63	0.30	1.00E+07
90th percentile	0.80	630	0.60	217	0.60	2.00E+07

Figures

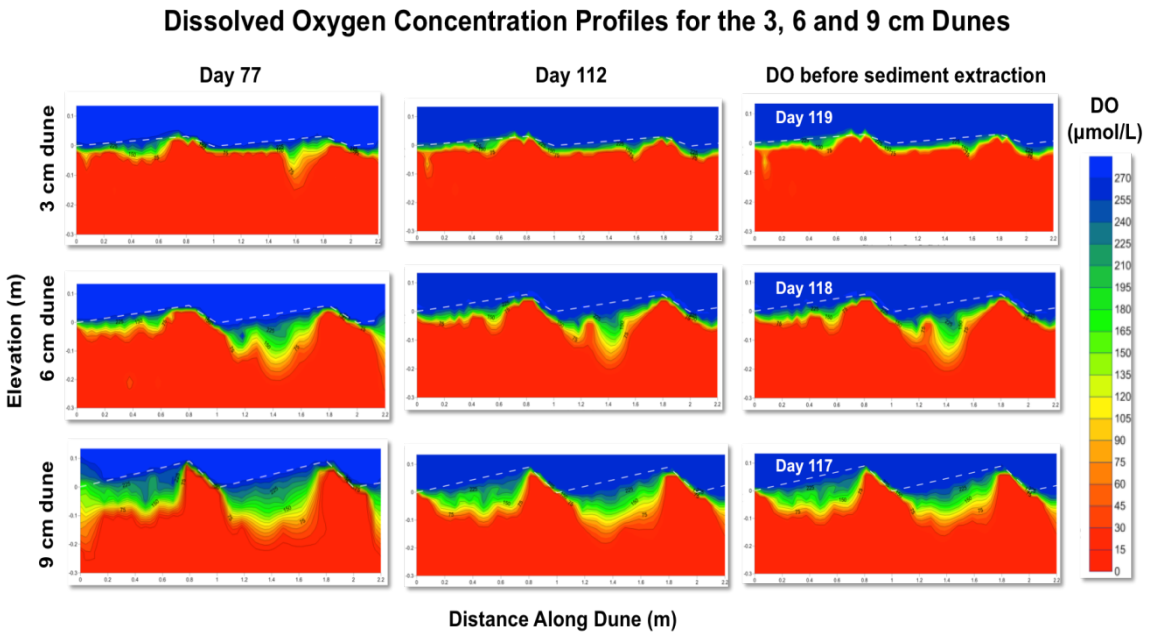

Figure 1: Dissolved oxygen (DO) within the 3, 6, and 9 cm dune measured on days 77, 112, and 117-119. The last day of geochemical analysis took place on day 112 and sediment extraction took place on days 117, 118, and 119 for the 9, 6, and 3 cm dune respectively. DO concentrations on day 112 were used in statistical analysis as a predictor variable for N_2O generation.

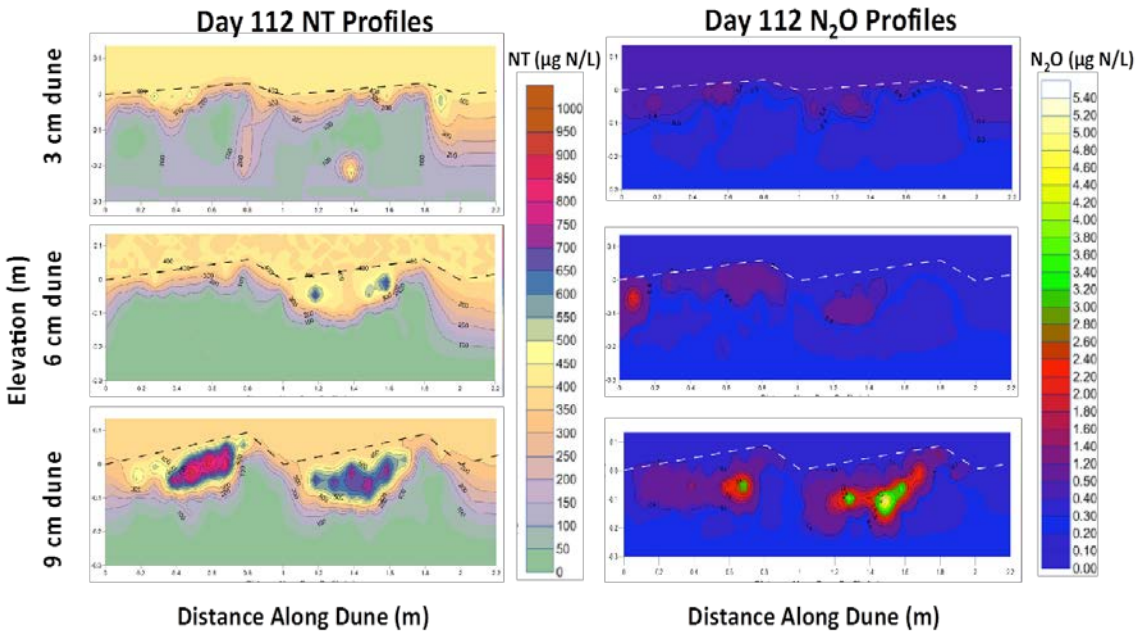

Figure 2: Geochemical profiles within each dune on day 112. Distribution of NT (NO_3^- + NO_2^- + NH_3) (right) and N_2O (left) within the 3, 6, and 9cm dunes on day 112. Concentrations of NT and N_2O obtained on day 112 were used in statistical evaluation using N_2O as the response variable and NT as a predictor variable.

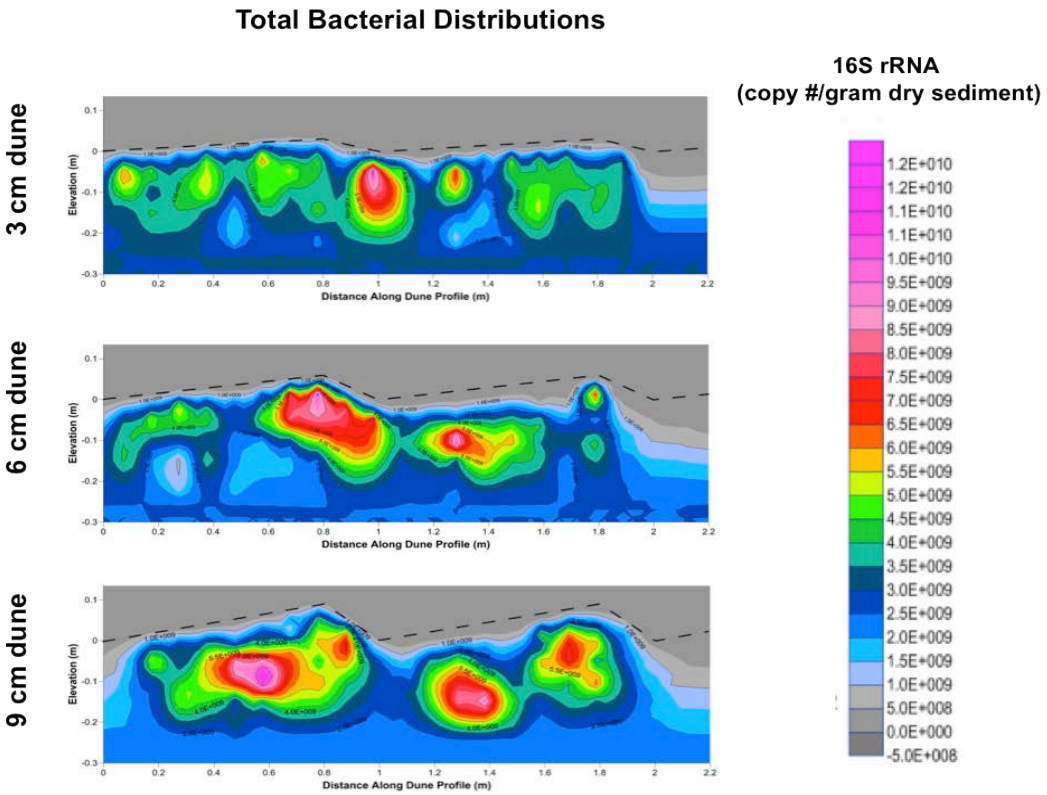

Figure 3: Total bacterial distribution profiles within the 3, 6, and 9 cm dune measured as 16S rRNA copy #/ gram dry sediment.

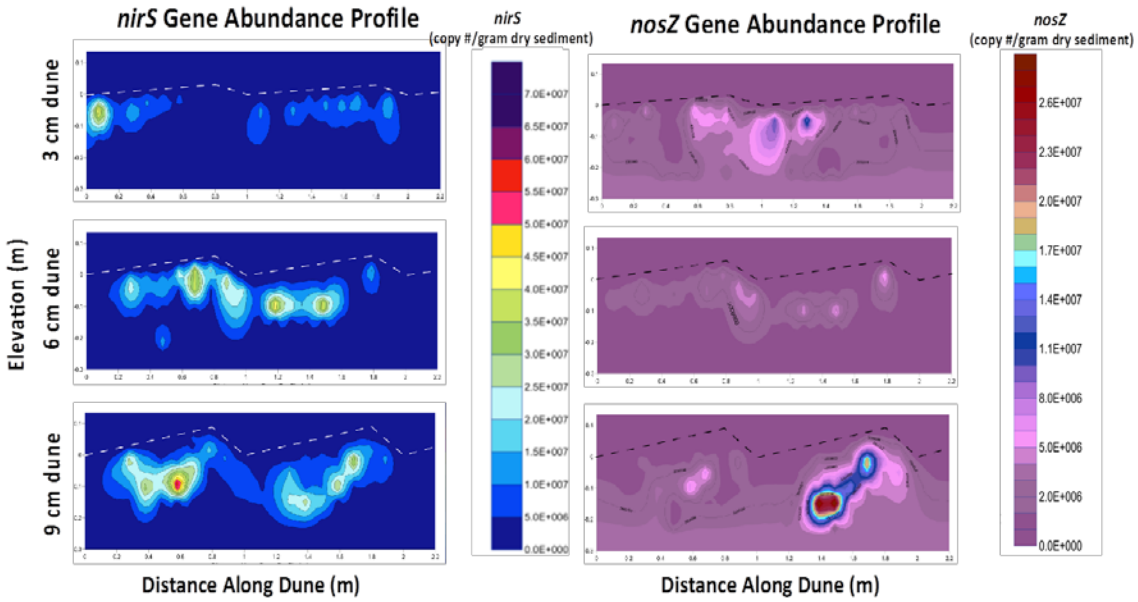

Figure 4: nirS gene abundance (right) and nosZ gene abundance (left) distribution profiles within the 3, 6, and 9 cm dune measured as copy #/gram dry sediment.

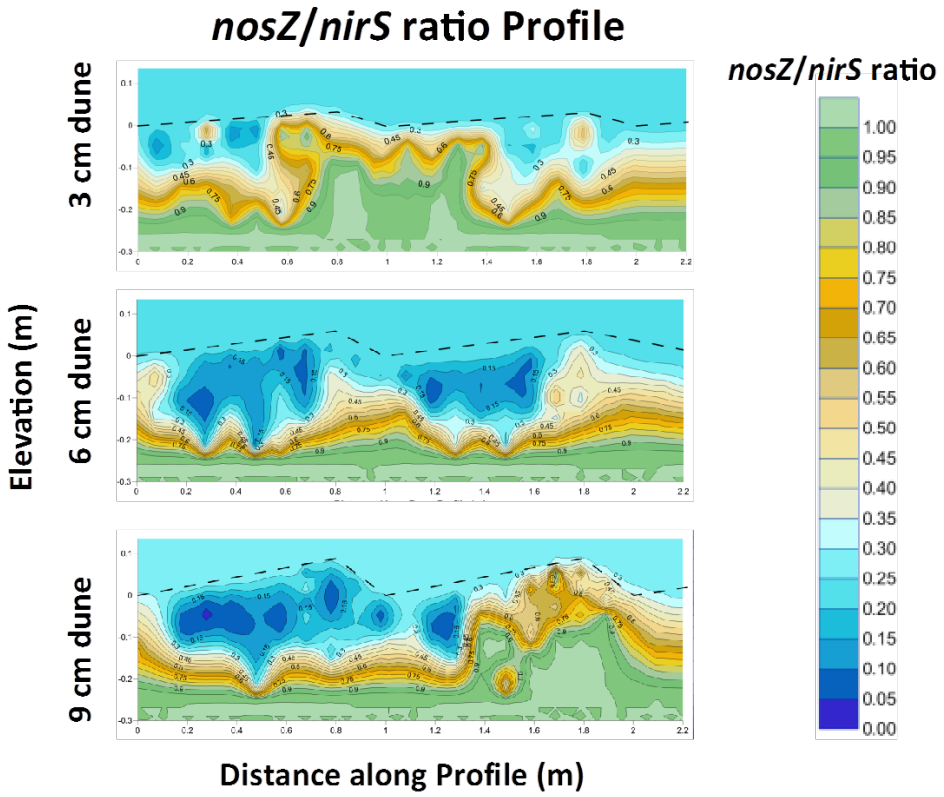

Figure 5: Distribution of the ratio of the relative abundance of *nosZ* to the relative abundance of *nirS* (*nosZ*/*nirS*) within the 3, 6, and 9 cm dune.

APPENDIX A

Supplementary Tables

Table A.1: Spearman Rank Correlation for modeling variables. Asterisks represent p-values: * =0.0000, ** ≥ 0.001, * ≥0.01**

	N2O	NT	DO	nirS	nosZ	nosZ/nirS	height
N_2O							
NT	0.66***						
DO	0.50***	0.62***					
nirS	0.59***	0.36***	0.44***				
nosZ	0.35***	0.25**	0.18*	0.65***			
nosZ /nirS	-0.28***	-0.14*	-0.34***	-0.42***	0.38***		
height	0.39***	0.28***	0.38***	0.24**	0.05	-0.20*	
dune	-0.24**	0.05	0.07	-0.02	0.29***	0.39***	-0.07

Table A.2: First Round of AICc Model Selection. The first round of AICc model selection included evaluation of all possible predictor variables using maximum likelihood and nlme. No spatial variance structures were applied.

Model Name	Predictor Variable Combination	AICc (using ML)
A_3	NT + *nirS* + (NT**nirS*)	103.99
A_14_B	NT + DO + *nirS* + (NT*DO) + (NT**nirS*)	105.26
A_15	NT + DO + *nirS* + (NT**nirS*)	105.34
A_2	NT + *nirS*	107.75
A_17	NT + DO + *nirS*	109.54
A_14	NT + DO + *nirS* + (NT*DO)	111.26
A_16	NT + DO + *nirS* + (DO**nirS*)	111.59
C_5	NT + *nosZ/nirS* + (NT**nosZ/nirS*)	141.45
C_8	NT + DO + *nosZ/nirS* + (NT*DO)	142.41
C_7	NT + DO + *nosZ/nirS* + (NT*DO**nosZ/nirS*)	142.22
D_2	NT + DO + (NT*DO)	144.27
C_4	NT + *nosZ/nirS*	144.40
C_6	NT + DO + *nosZ/nirS*	146.09
A_1	NT	146.87
D_1	NT+DO	147.60
B_1	DO + *nirS*	154.21
B_2	DO + *nirS* + (*nirS**DO)	156.30
A_11	*nirS*	170.45
B_5	DO	189.30
C_2	DO + *nosZ/nirS*	190.44
C_3	DO + *nosZ/nirS* + (DO**nosZ/nirS*)	190.76
C_1	*nosZ/nirS*	225.09

Table A.3: Second Round of AICc Model Selection. A second round of AICc model selection considered the addition of dune height (amplitude), dune as an ordered factor, as well as the interactions between the two variables within the models of interest from the first round of AICc selection. Using the nlme, the maximum likelihood function was applied and no spatial variance structures were considered.

Model Name	Predictor Variable Combination	AICc (using ML)
A_14_B_dune_height_C	NT + DO + *nirS* + (NT**nirS*) + (NT*DO) + dune + height + (dune*height)	67.21
A_15_dune_height_B	NT + DO + *nirS* + (NT**nirS*) + dune + height + (dune*height)	72.46
A_14_B_dune_height_A	NT + DO + *nirS* + (NT*DO) + dune + height + (dune*height)	75.26
A_14_B_dune_height_B	NT + DO + *nirS* + (NT**nirS*) + (NT*DO) + dune + height	76.52
A_3_dune	NT + *nirS* + (*nirS**NT) + dune	80.97
A_15_dune_height	NT + DO + *nirS* + (NT**nirS*) + dune + height	81.42
A_3_dune_height	NT + *nirS* + (*nirS**NT) + dune + height	89.49
A_15_height	NT + DO + *nirS* + (NT**nirS*) +(NT*DO) + height	90.55
A_15_dune	NT + DO + *nirS* + (NT**nirS*) + dune	91.40
C_8_dune_height_B	NT + DO + *nosZ/nirS* + (NT*DO) + dune + height+ (dune*height)	107.96
C_8_dune_height_C	NT + DO + *nosZ/nirS* + (NT**nosZ/nirS*) + (NT*DO) + dune + height + (dune*height)	108.52
C_8_dune_hieght	NT + DO + *nosZ/nirS* + (NT*DO) + dune + height	113.75
C_5_dune_height_B	NT + *nosZ/nirS* + (NT**nosZ/nirS*) + dune + height + (dune*height)	115.56
C_5_dune_height	NT + *nosZ/nirS* + (NT**nosZ/nirS*) + dune + height	120.16
C_8_dune	NT + DO + *nosZ/nirS* + (NT*DO) + dune	129.77
C_5_dune	NT + *nosZ/nirS* + (NT**nosZ/nirS*) + dune	132.26

Table A.4: Third Round of AICc Model Selection. Due to the physical parameters of the flume, the necessity for the application of spatial covariance structures was evaluated. We applied spherical, Gaussian, linear, rational, and exponential spatial covariance structures as well as unequal variance by dune and independent (null). Using nlme, the restricted maximum likelihood function was applied and AICc model selection determined the best application for our model.

Model Name	Predictor Variable Combination	AICc (using REML)
A_14_B_unequal	**NT + DO + *nirS* + (NT**nirS*) + (NT*DO) + dune + height + (dune*height)**	**101.41**
A_14_B_ratio	NT + DO + *nirS* + (NT**nirS*) + (NT*DO) + dune + height + (dune*height)	103.52
A_14_B_exp	NT + DO + *nirS* + (NT**nirS*) + (NT*DO) + dune + height + (dune*height)	103.98
A_14_B_null	NT + DO + *nirS* + (NT**nirS*) + (NT*DO) + dune + height + (dune*height)	107.76
A_14_B_gau	NT + DO + *nirS* + (NT**nirS*) + (NT*DO) + dune + height + (dune*height)	112.37
A_14_B_sphere	NT + DO + *nirS* + (NT**nirS*) + (NT*DO) + dune + height + (dune*height)	112.37
A_14_B_lin	NT + DO + *nirS* + (NT**nirS*) + (NT*DO) + dune + height + (dune*height)	112.37

Table A.5: Analysis of Variance for *nosZ*/*nirS* and N_2O. Though not the best predictor variable for N_2O generation within our system, we were still interested in its relationship with the relative abundance of *nosZ* to *nirS* (*nosZ*/*nirS* ratio). We therefore applied nlme along with a spherical spatial covariance structure (as determined by AICc model selection using the restricted maximum likelihood function)

Model Parameter	Coefficient	Standard Error	95% Confidence Intervals	p-value
Intercept	-0.01	0.08	(-0.17, 0.15)	0.897
nosZ/nirS	-0.27	0.10	(-0.47, -0.08)	0.007

APPENDIX B

Supplementary Methods

Water Sample Collection from N_2O and Water Chemistry Analysis

Glass flat bottom GC headspace vials and aluminum crimp caps with septa (PTFE/Si) (20 ml/ 20 mm) (Agilent Technologies, New Castle, DE) were acid washed (10% HCl) before obtaining an initial mass. Headspace vials were overfilled with water previously degassed with ≥ 99.999% argon (Ar) (argon, UHP, Norco, Boise, ID) (5 psi/1L water/covered with parafilm/~10 minutes) and immediately capped. Vials were then inverted and evacuated by inserting two 22-guage needles, one with a constant stream of Ar and the other acting as a vent to allow the degassed water to escape. After the water was evacuated a second mass was obtained. A 1" 16-gauge needle (PrecisionGlide® needle, BD, Franklin Lakes, NJ) attached to a 5 ml plastic syringe (luer lock™ tip, BD, Franklin Lakes, NJ) was used to vent any excess gas pressure while a second 1" 16-gauge needle attached to a 5 ml plastic syringe injected 6 drops of 6 N sulfuric acid (decreasing final pH of the sample to <2.0) into each vial. A third mass was then obtained. Headspace vials were stored inverted in small water filled containers between preparation steps and during transport to the flume. Standards for 0.1 ppm N_2O and 1.0 ppm N_2O were prepared as described above using the necessary gas concentration for displacement of Ar saturated water.

Microbial Community Analysis

Quantitative PCR (qPCR) was employed to quantify total bacterial densities (measured as total Eubacterial 16S gene copy #/g dry sediment) as well as denitrifying genes; *nirS*, *nirK*, and *nosZ* (measured as copy #/gram dry sediment). The standard for 16S rRNA gene amplification was prepared from *Bacillus subtilis* using the forward primer 27F (5'-AGAGTTTGATCCTGGCTCAG-3') and reverse primer 1492R (5'-

TACGGYTACCTTGTTACGACTT-3') (Polz and Cavanaugh 1998). Standard curves for amplification of *nirS*, *nirK*, and *nosZ* were established using gene fragments from *Pseudomonas aeruginosa* PAO1 A+B+, a CF161 isolate, and *Paracoccus denitrificans* respectively. Amplicons were gel-purified using the Wizard® SV Gel and PCR Clean-up System (Promega, Madison, WI), cloned into plasmid pGEM-T easy Vector (3015 bp, Promega, Madison, WI), and transformed into *Escherichia coli* JM109 competent cells. Plasmid DNA was extracted using the QIAprep® Spin Miniprep Kit (QIAGEN, Venlo, Netherlands) and concentration determined with a NanoDrop3300 Fluorospectrometer. 10-fold serial dilutions of the plasmids were used to generate standard curves. qPCR reactions were performed in triplicate for each targeted gene randomly on thirty percent of the samples. Two no template control (NTC) treatments were included in all runs. All reactions were performed in 7300 Real Time PCR System (Applied Biosystems, Waltham, MA).

Total bacterial PCR amplification was performed in a total volume of 12.5 μL using the following reaction chemistry; 6.25 μL of ABsolute Blue QPCR ROX (Thermo-Scientific, Waltham, MA), 0.5 μL (0.8 μM final concentration) (each) forward and reverse primers, 0.25 μL (0.2 μM final concentration) of the probe and 4 μL PCR qualified water (Quality Biological, INC, Gaithersburg, MD). Thermal cycling conditions for 16S rRNA gene amplification were 50^{o} C for 2 minutes, 95^{o} C for 5 minutes, followed by 40 cycles of 30 s at 95^{o} C, 30 s at 56^{o} C, and 30 s at 72^{o} C. Standard curves were linear across 5 orders of magnitude ($2.09x10^{3}$ to $2.09x10^{8}$ gene copies/μL of extracted DNA) (average efficiency: 99%, average R^{2}: 0.996, average slope: -3.34).

PCR amplification of the denitrifying genes *nirS*, *nirK*, and *nosZ* were performed in a reaction mixture that included the following: 12.5 µL of QuantiTect SYBR Green PCR master mix (QuantiTect SYBR green PCR Kit, QIAGEN, France), 1.0 µL (0.5 µM final concentration) (each) forward and reverse primers, 2.5 µL (.004 µM final concentration) T4 Gene 32 Protein (New England BioLabs, Ipswich, MA), a respective volume providing final $MgCl_2$ concentrations of 3.8 mM for *nirS* and *nirK* reactions and 5.0 mM for *nosZ* reactions, 1.0 µL of the template DNA (diluted to <2 ng/µL, 0.5 ng/µL, and <1 ng/µL for *nirS*, *nirK*, and *nosZ* respectively) and PCR water to achieve a total reaction volume of 25 µL . Thermal cycling conditions for each gene target included an initial heat activation at 95^{o}C for 15 minutes followed by 6 touchdown cycles at 95^{o} C for 15 s, 65^{o}C for 30 s (-1^{o}C cycle^{-1}), and 72^{o}C for 30 s. This was then followed by 40 cycles of denaturation, elongation and data collection that was the same for all gene targets; 95^{o}C for 15 s, 72^{o}C for 30 s, and 80^{o}C for 30 s respectively, however annealing temperatures post touchdown were 60.2 ^{o}C, 59.0 ^{o}C, and 60.0 ^{o}C for the *nirS*, *nirK*, and *nosZ* respectively. Each qPCR run was followed by a dissociation curve analysis. Standard curves were linear across 5 orders of magnitude (($3.29x10^2$ to $3.29x10^7$ gene copies/µL of extracted DNA) (average efficiency: 99%, average R^2: 0.995, average slope: -3.35)), (($1.19x10^2$ to $1.19x10^7$ gene copies/µL of extracted DNA) (average efficiency: 100%, average R^2: 0.995, average slope: -3.31)) and (($2.03x10^2$ to $2.03x10^7$ gene copies/µL of extracted DNA) (average efficiency: 100%, average R^2: 0.996, average slope: -3.32)) for *nirS*, *nosZ*, and *nirK*, respectively.